Video Article

A Time-lapse, Label-free, Quantitative Phase Imaging Study of Dormant and Active Human Cancer Cells

Jing Huang*[1,2], Peng Guo*[1,2], Marsha A. Moses[1,2]

[1]Vascular Biology Program, Boston Children's Hospital

[2]Department of Surgery, Harvard Medical School and Boston Children's Hospital

*These authors contributed equally

Correspondence to: Marsha A. Moses at Marsha.Moses@childrens.harvard.edu

URL: https://www.jove.com/video/57035
DOI: doi:10.3791/57035

Keywords: Cancer Research, Issue 132, Quantitative phase imaging, holographic microscopy, tumor dormancy, tumor angiogenesis, cell phenotype, cell morphology, cell migration, cell cycle, osteosarcoma

Date Published: 2/16/2018

Citation: Huang, J., Guo, P., Moses, M.A. A Time-lapse, Label-free, Quantitative Phase Imaging Study of Dormant and Active Human Cancer Cells. *J. Vis. Exp.* (132), e57035, doi:10.3791/57035 (2018).

Abstract

The acquisition of the angiogenic phenotype is an essential component of the escape from tumor dormancy. Although several classic *in vitro* assays (*e.g.*, proliferation, migration, and others) and *in vivo* models have been developed to investigate and characterize angiogenic and non-angiogenic cell phenotypes, these methods are time and labor intensive, and often require expensive reagents and instruments, as well as significant expertise. In a recent study, we used a novel quantitative phase imaging (QPI) technique to conduct time-lapse and labeling-free characterizations of angiogenic and non-angiogenic human osteosarcoma KHOS cells. A panel of cellular parameters, including cell morphology, proliferation, and motility, were quantitatively measured and analyzed using QPI. This novel and quantitative approach provides the opportunity to continuously and non-invasively study relevant cellular processes, behaviors, and characteristics of cancer cells and other cell types in a simple and integrated manner. This report describes our experimental protocol, including cell preparation, QPI acquisition, and data analysis.

Video Link

The video component of this article can be found at https://www.jove.com/video/57035/

Introduction

One of the earliest checkpoints in the development and progression of a solid tumor is the acquisition of the angiogenic phenotype, a hallmark of cancer. This progression involves a variety of biochemical and molecular processes[1,2,3]. A technical challenge in the study of this key step in tumor progression is the lack of tools to continuously and quantitatively characterize and differentiate between angiogenic and non-angiogenic phenotypes of live cancer cells in an unbiased manner. The traditional assays being used to investigate the cellular behaviors of angiogenic and non-angiogenic cells usually require expensive reagents and instruments, for example, cell proliferation/migration assays[4,5,6,7,8,9,10,11,12,13,14] or complementary *in vivo* evaluations[4,5,6,8,15,16], as well as requiring significant expertise and intensive time and labor consumption.

Recently, quantitative phase imaging (QPI) has emerged as a novel technique that enables time-lapse and labeling-free assessment of a variety of cell morphology and behavior parameters[17,18,19,20,21,22]. Unlike conventional optical microscopy, QPI quantifies variations of phase shift pixel by pixel after light passes through an optical object, and reconstructs a holograph with converted optical thickness and volume, thus enabling the direct analysis of live cells and the following features: (1) quantitative imaging, (2) non-invasive and time-lapse imaging, (3) label-free imaging, and (4) simultaneous multi-parameter imaging. These features make QPI a powerful tool to assess and understand pathological processes at cellular level.

In a recent study, we utilized QPI to quantitatively characterize and differentiate between angiogenic KHOS-A and non-angiogenic KHOS-N phenotypes of human osteosarcoma cells in a systematic and quantitative manner, combining analyses of cell morphology, proliferation, and motility[23]. Using image analysis software, a panel of cell morphological and behavior parameters were quantitatively compared between angiogenic and non-angiogenic human osteosarcoma cells and five characteristic differences were identified between these two phenotypes. This novel approach provides an integrated and quantitative platform for assessing a variety of biologically relevant cellular characteristics.

Protocol

All the methods described here have been approved by the Boston Children's Hospital Institutional Biosafety Committee.

1. Cell Preparation

1. **Thawing KHOS-A and -N cells**
    1. Warm up culture medium, *i.e.*, Dulbecco's modified Eagle medium supplemented with 10% (vol/vol) fetal calf serum (FBS) and 1% (vol/vol) penicillin/streptomycin.
    2. Take the cryogenic vials of cells from the liquid nitrogen tank, immerse the bottom of the vials into warm water in a 37 °C water bath, and gently shake the cryogenic vials to accelerate the thawing process. Keep the lid of cryogenic vials from contacting water in order to avoid contamination. As soon as cells are thawed, sterilize the cryogenic vial by spraying 70% ethanol solution and wiping the vial.
    3. In a laminar flow hood, immediately aspirate the cell suspension from the cryogenic vial, and gently suspend in 10 mL warmed culture medium (described in 1.1.1). Centrifuge cell suspensions at approximately 200 x g for 5 - 7 min.
    4. Resuspend the cell pellet with 10 mL warmed culture medium, and transfer into a T75 flask. Gently pipette several times to suspend cells evenly using a 10-mL pipet.
    5. Place the flask into a 37 °C incubator with 5% (vol/vol) CO_2 and humidified atmosphere. Allow cells to attach for at least 12 h.
    6. Incubate cells for approximately 3 - 7 days until 80 - 100% confluent. Change the culture medium every 2 - 3 days.

2. **Splitting KHOS-A and -N cells**
    1. Remove the culture media from the flask.
    2. Wash the cells with 5 mL sterile PBS (1x) without calcium and magnesium, to remove non adherent cells or fraction.
    3. Add 1 mL 0.05% Trypsin-EDTA solution into the flask, and briefly swirl the flask to ensure that the trypsin-EDTA is dispersed evenly.
    4. Incubate the flask for 2 - 3 min in a 37 °C incubator or 3 - 5 min at room temperature. Check the cells under a microscope at approximately 400x magnification to make sure that the cells are rounded up and detached.
    5. Once the cells are detached, add 10 mL culture medium and gently pipette the medium up and down several times to break up cell aggregates into a single cell suspension using a 10 mL pipet.
    6. Count cells using a cell counter. Seed the cell suspension into new T75 flasks at a density of 2×10^6 cells or a ratio of 1:4.
    7. Allow cells to grow to 80 - 100% confluence before seeding for the QPI experiment.

3. **Seeding KHOS-A and -N cells for QPI**
    1. Seed KHOS-A and -N cells in 6-well plates at the density of 50,000 - 300,000 cells/well with 5 mL culture medium after counting with a cell counter.
    NOTE: The seeding density is dependent on the cell proliferation rate, and the imaging time period in order to have <100% confluence during imaging acquisition.
    2. Incubate cells for at least 12 h to allow attachment.
    3. Change the medium with fresh media before conducting QPI.

2. QPI Acquisition

1. **Cover slip set up**
    1. Clean the cover slip by rinsing several times with running deionized water and sterilize with 75% ethanol solution by immersion for 15 min. Put the cover slip into a sterile laminar flow hood to dry.
    2. Carefully place the cover slip onto a 6-well plate to avoid obvious bubbles. Ensure that the bottom of the cover slip is immersed in the culture media (minimum 5 mL/well).
    3. Place the plate into the incubator (37 °C, 5% CO_2, and humidified atmosphere) to equilibrate for at least 15 min. If fog forms on the cover slip, use a sterile cotton swab to wipe it clean.

2. **Imaging cells with a microscope**
    1. Open the software to initialize the system, including self calibration of exposure time, pattern contrast, and hologram noise. Make sure the values are acceptable (shown in green or yellow range).
    2. Place the 6-well plate onto the stage of the QPI microscope.
    3. Click "Live Capture," and select "Manual" in "Software focus." Coarsely focus the phase images of cells by adjusting the work distance in "Microscope setting" to obtain outlines for cells in phase images. Change to "Automatic" in "Software focus."
    4. Click "New experiment" to create a new experiment. Start with the selection of image acquisition positions using the mouse or the arrow keys on the numerical pad. Click "Remember" after each selection. Normally 3 - 5 locations for each sample are selected.
    5. Set up the imaging intervals and time period in the "Timelapse" section.
    NOTE: To track cancer cells clearly, the intervals should be shorter than 5 min. 48 hours is set as the time period for the combination QPI analysis.
    6. Start the experiment by clicking "Capture," which will automatically focus and acquire the images at the setting time points.

3. Data Analysis

1. **Cell morphology analysis**
    1. Click "Identify cells." Adjust the numeric setting for "Background threshold" so that cell areas are separated well from background noise. Adjust the setting number for "Object size" to make sure that each cell has one nucleus. Maintain consistent parameters for samples that need to be compared, as these may affect the final area and volume measurements. Manually modify cell segments by using "Manual changes," if needed.

2. Use the "Analyze data" function in the software to analyze cells. Start a new data analysis by clicking "New analysis." Drag selected images into the "Source frames" tab and cell morphology parameters including cell area (μm^2), optical thickness (µm), and volume (μm^3) for every individual cell. Choose scatter plot or histogram mode and export data as tables or figures.

2. **Cell proliferation analysis**
    1. Select at least 5 images for the different time points of interest (*e.g.*, initial, 12 h, 24 h, 36 h, and 48 h). Record cell numbers that are provided by the software.
    2. To estimate the doubling time, plot cell numbers after normalizing with the initial numbers and fit with exponential growth curves.

3. **Cell motion analysis**
    1. Use the "Track cells" function in the software. Click "New analysis" to start a new data analysis. Drag series of images for a selected time period (*e.g.*, 4 h after 24 h incubation) into the "Source frames" tab. Randomly choose 10 - 30 cells by clicking cells under the "Add cells" selection mode. Exclude the cells at the edges and those moving out of the field of view.
    2. Carefully check the tracking in the series of images. In the event that the system loses track of a cell or tracks the wrong cell, manually adjust the tracking cell by clicking "Identify" to identify cells or clicking "Modify location" under the "Select" mode to modify the cell location.
    3. Choose rose plot of cell trajectories in "Plot movement" or plot for the other motion-related parameters in "Plot features," such as motility speed (µm/h), motility (µm), migration (µm), and migration directness. Export Data as tables or figures.

Representative Results

Figure 1 depicts a typical cell morphology characterization. Images are presented as holographs (**Figure 1A-B**) and 2D images (**Figure 1C-D**). Optical cell thicknesses (calculated from the refractive index and optical path length) are quantified via line profile or a whole cell measurement. Scatter plots of the area and thickness of KHOS-A and KHOS-N cells measured for a whole cell were plotted, as in **Figure 1E-G**, where these two phenotypes displayed different distribution patterns. The average numbers from the histogram (**Figure 1H-M**) or the exported files demonstrated that KHOS-A cells have smaller cell areas and greater thicknesses than KHOS-N cells.

Using the cell counter function, cell proliferation profiles were obtained (**Figure 2**). These did not show a significant difference between KHOS-A and -N cells. In addition, the cell doubling time could be estimated from the proliferation curve (*i.e.*, 24 - 26 h), which also did not show significant differences.

Figure 3A-D shows the typical tracking of KHOS-A and -N cells in non-directional (random) motion mode and the corresponding trajectories. The average cell motility (**Figure 3E-F)**, motility speed **(Figure 3G-H)**, migration distance **(Figure 3I-J)**, and migration directness **(Figure 3K-L)** were plotted versus recording time. Compared to KHOS-N cells, KHOS-A cells showed greater motility speed, resulting in longer motility and migration distance.

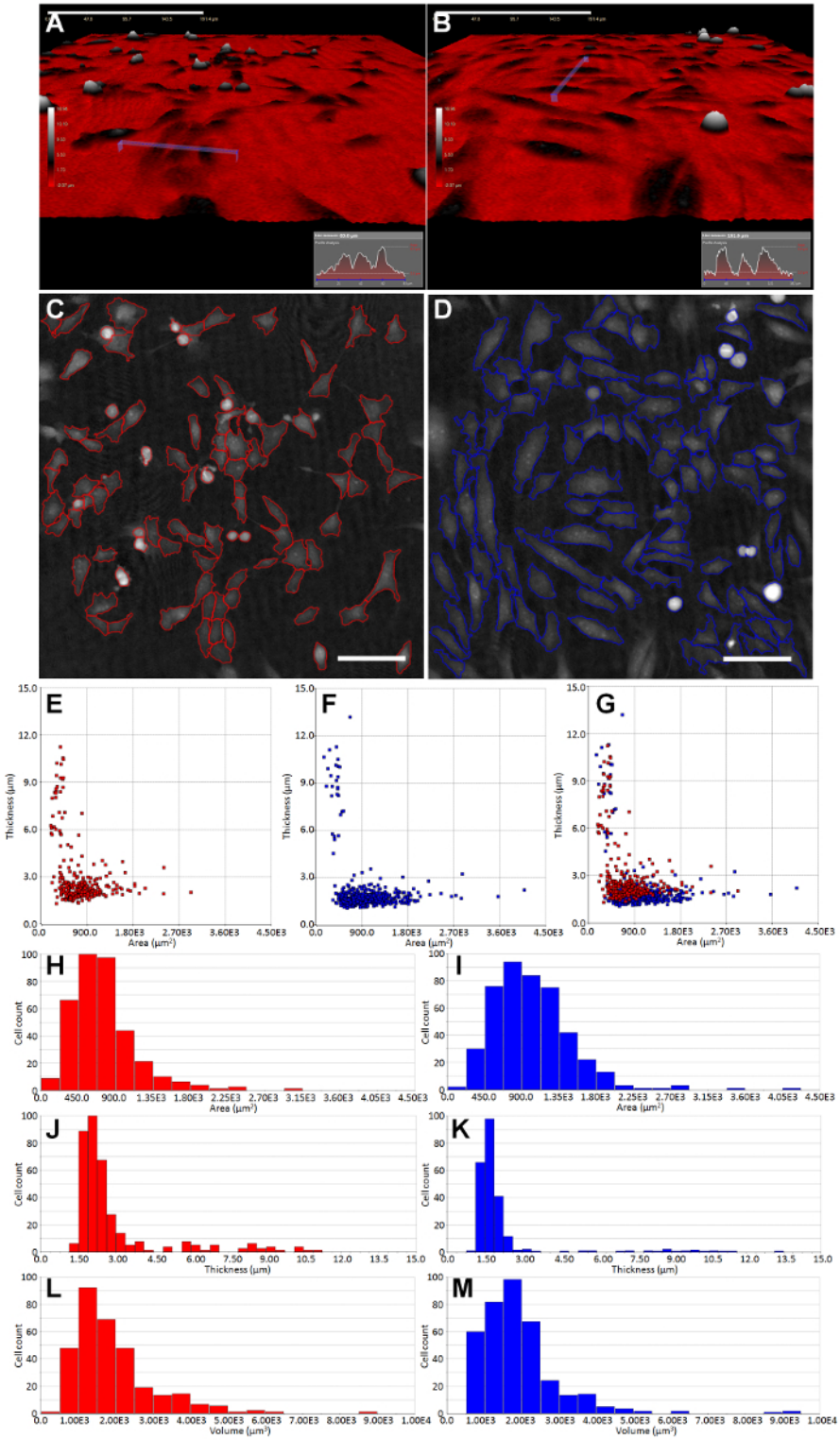

Figure 1: Cell morphology characterization. (A-B) Representative holographs of KHOS-A **(A)** and -N cells **(B)** by quantitative phase imaging. Scale bar is 191.4 µm. Insets at the right bottom corner show the quantitative line profile of optical thickness for the blue line drawn in the images. **(C-D)** Representative QPI images of cell segmentation for KHOS-A **(C)** and -N cells **(D)**. Scale bar is 100 µm. Cells at the edges were excluded for the quantification. **(E-G)** Measured thickness versus area for individual cells of KHOS-A **(E)** and -N cells **(F)**. Each dot represents an individual cell (n = 200 - 300). The overlap plot **(G)** shows significantly different dispersion patterns for KHOS-A and -N cells. **(H-M)** Histograms of cell thickness **(H-I)**, area **(J-K)**, and volume **(L-M)** distribution for KHOS-A **(H, J, L)** and -N cells **(I, K, M)**. Please click here to view a larger version of this figure.

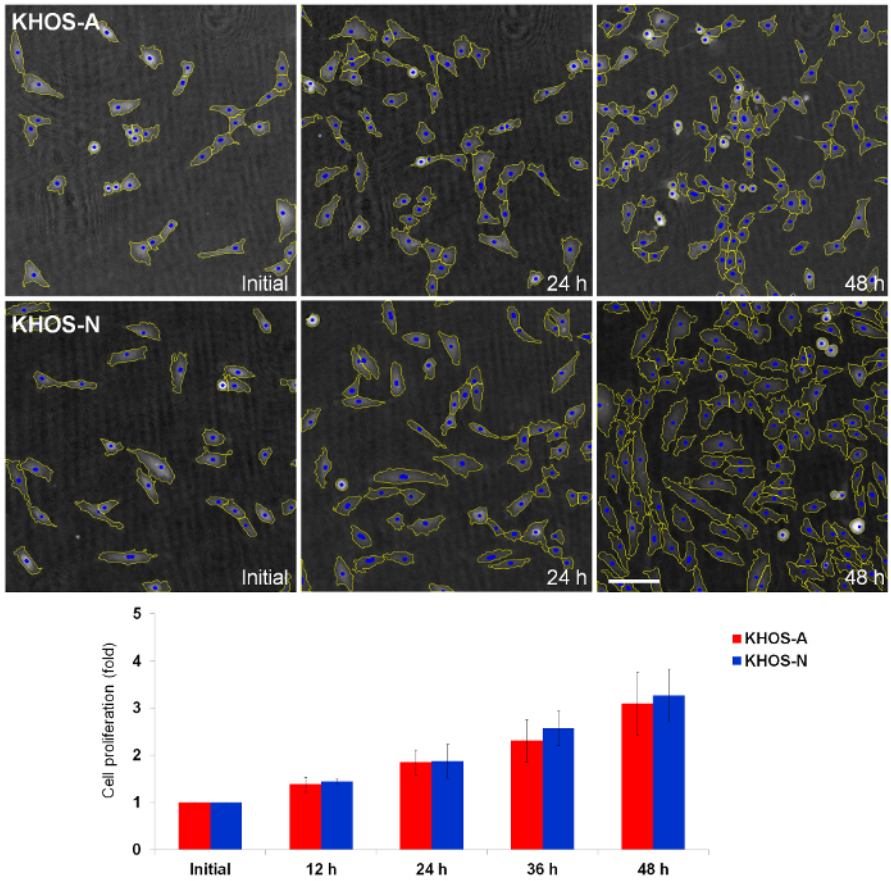

Figure 2: Cell proliferation characterization. The upper panel shows representative cell segmentation for counting cell numbers. Scale bar is 100 µm. The bottom panel shows the corresponding calculated cell proliferation rate. Data is presented as mean ± standard deviation. Student's t test (unpaired, two-tailed) was used for statistical analyses. Test results were considered significant when p <0.05. Please click here to view a larger version of this figure.

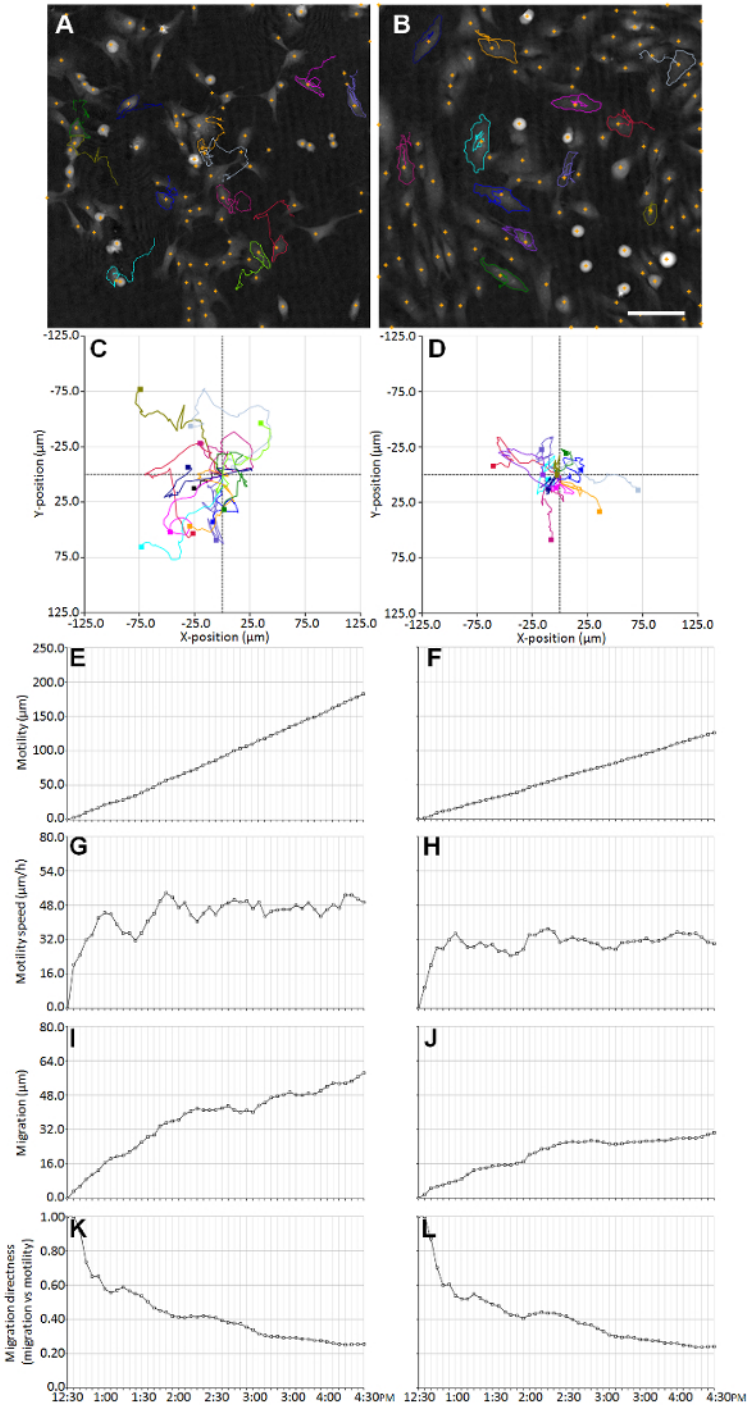

Figure 3: Cell motion characterization. (A-B) Representative cell tracking images for KHOS-A **(A)** and -N **(B)** cells. Scale bar is 100 µm. Selected cells are outlined with different colors. Cell motility recorded in a 4 h time period is presented with the corresponding colored line. **(C-D)** Cell trajectories of KHOS-A **(C)** and -N **(D)** cells plotted from the point of origin (0,0). Each line represents an individual cell. KHOS-A cells showed a more dispersed pattern compared with KHOS-N cells (n = 10). **(E-L)** Recorded quantitative parameters during the investigated time period for cell motion of KHOS-A **(E, G, I, K)** and -N **(F, H, J, L)** cells, including cell motility **(E-F)**, motility speed **(G-H)**, migration distance **(I-J)**, and migration directness **(K-L)**. Please click here to view a larger version of this figure.

Discussion

In this study, we describe an *in vitro*, non-invasive, and label-free method using QPI to quantitatively characterize the angiogenic and non-angiogenic phenotypes of human osteosarcoma cells. Multiple cellular parameters have been analyzed simultaneously by this integrated, high-throughput method, including cell area, cell thickness, cell volume, proliferation rate, doubling time, migration directness, motility speed, migration, and motility.

Compared with the conventional assays that assess cell morphology and cell behaviors, this method not only saves time and labor, but also provides more accurate and detailed information. For example, the location of the QPI system (inside of the cell incubator) reduces the disturbances from environmental changes such as photographing in an ambient environment (room temperature and atmosphere)[23]. In addition, optical cell thickness and volume, converted from phase shift, could be obtained with QPI, whereas only cell area is measured by the traditional cell imaging process. This feature of QPI generates more detailed information for quantitative comparisons of different cell phenotypes.

Proper seeding density of the cells of interest is critical in the current method. During the imaging acquisition phase, cells are expected to be less than a confluent monolayer due to the limitation of this coherent QPI technique that imaging acquisition could only be performed with one focus panel, which may lose partial information in the z direction (*i.e.*, overlaid cells). In addition, characterizations using QPI are limited to the 2D format, which is not optimal for cell invasion in the z direction in the extracellular matrix. Multiple preset focal lengths are needed for future QPI methodology development.

In addition to cell counting, QPI imaging also provides informative images for studying cell mitosis without additional labeling[21,23,24]. While cell division was recognized easily by the obvious decrease in cell area and volume, the ability to objectively and quantitatively define and differentiate cell cycle stages for single cells has yet to be established. This capability would significantly facilitate research with respect to cell analysis for stem cell differentiation, drug response, and cell cycle arrest.

Due to the advantages of being quantitative, label-free, and easy to use, this method may also have useful clinical applications[25,26,27,28,29,30]. For example, this system could be utilized in the characterization of heterogeneous cell populations, including dormant and active cells in human tumors. The characterized cell morphological and behavioral differences between dormant and active cancer cells can be potentially used to decipher the molecular mechanisms underlying tumor dormancy in human cancers.

Disclosures

No conflicts of interest declared.

Acknowledgements

The authors gratefully acknowledge the support of the Breast Cancer Research Foundation and the Advanced Medical Research Foundation.

References

1. Folkman, J. Angiogenesis in cancer, vascular, rheumatoid and other disease. *Nature Medicine.* **1** (1), 27-31 (1995).
2. Hanahan, D., & Folkman, J. Patterns and emerging mechanisms of the angiogenic switch during tumorigenesis. *Cell.* **86** (3), 353-364 (1996).
3. Harper, J., & Moses, M. A. Molecular regulation of tumor angiogenesis: mechanisms and therapeutic implications. *EXS.* (96), 223-268 (2006).
4. Naumov, G. N. *et al.* A model of human tumor dormancy: an angiogenic switch from the nonangiogenic phenotype. *Journal of the National Cancer Institute.* **98** (5), 316-325, (2006).
5. Fang, J. *et al.* Matrix metalloproteinase-2 is required for the switch to the angiogenic phenotype in a tumor model. *Proceedings of the National Academy of Sciences of the United States of America.* **97** (8), 3884-3889 (2000).
6. Almog, N. *et al.* Transcriptional switch of dormant tumors to fast-growing angiogenic phenotype. *Cancer Research.* **69** (3), 836-844, (2009).
7. Hu, J. *et al.* Gene expression signature for angiogenic and nonangiogenic non-small-cell lung cancer. *Oncogene.* **24** (7), 1212-1219, (2005).
8. Harper, J. *et al.* Repression of vascular endothelial growth factor expression by the zinc finger transcription factor ZNF24. *Cancer Research.* **67** (18), 8736-8741, (2007).
9. Jia, D. *et al.* Transcriptional repression of VEGF by ZNF24: mechanistic studies and vascular consequences in vivo. *Blood.* **121** (4), 707-715, (2013).
10. Jia, D., Huang, L., Bischoff, J., & Moses, M. A. The endogenous zinc finger transcription factor, ZNF24, modulates the angiogenic potential of human microvascular endothelial cells. *FASEB journal: official publication of the Federation of American Societies for Experimental Biology.* **29** (4), 1371-1382, (2015).
11. Almog, N. *et al.* Prolonged dormancy of human liposarcoma is associated with impaired tumor angiogenesis. *FASEB journal: official publication of the Federation of American Societies for Experimental Biology.* **20** (7), 947-949, (2006).
12. Almog, N. *et al.* Consensus micro RNAs governing the switch of dormant tumors to the fast-growing angiogenic phenotype. *PloS One.* **7** (8), e44001, (2012).
13. Satchi-Fainaro, R. *et al.* Prospective identification of glioblastoma cells generating dormant tumors. *PloS One.* **7** (9), e44395, (2012).
14. Almog, N. *et al.* Transcriptional changes induced by the tumor dormancy-associated microRNA-190. *Transcription.* **4** (4), 177-191 (2013).
15. Gao, D., Nolan, D. J., Mellick, A. S., Bambino, K., McDonnell, K., & Mittal, V. Endothelial progenitor cells control the angiogenic switch in mouse lung metastasis. *Science (New York, N.Y.).* **319** (5860), 195-198, (2008).
16. Folkman, J., Watson, K., Ingber, D., & Hanahan, D. Induction of angiogenesis during the transition from hyperplasia to neoplasia. *Nature.* **339** (6219), 58-61, (1989).
17. Popescu, G. *Quantitative phase imaging of cells and tissues.* McGraw-Hill: New York, (2011).
18. Lee, K. *et al.* Quantitative Phase Imaging Techniques for the Study of Cell Pathophysiology: From Principles to Applications. *Sensors.* **13** (4), 4170-4191, (2013).
19. Mir, M., Bhaduri, B., Wang, R., Zhu, R., & Popescu, G. Quantitative Phase Imaging. *Progress in Optics.* **57**, 133-217, (2012).
20. Marrison, J., Räty, L., Marriott, P., & O'Toole, P. Ptychography--a label free, high-contrast imaging technique for live cells using quantitative phase information. *Scientific Reports.* **3**, 2369, (2013).
21. Falck Miniotis, M., Mukwaya, A., & Gjörloff Wingren, A. Digital holographic microscopy for non-invasive monitoring of cell cycle arrest in L929 cells. *PloS One.* **9** (9), e106546, (2014).
22. Popescu, G. *et al.* Optical imaging of cell mass and growth dynamics. *AJP: Cell Physiology.* **295** (2), C538-C544, (2008).

23. Guo, P., Huang, J., & Moses, M. A. Characterization of dormant and active human cancer cells by quantitative phase imaging. *Cytometry. Part A: The Journal of the International Society for Advancement of Cytometry.* **91** (5), 424-432, (2017).
24. Mir, M., Bergamaschi, A., Katzenellenbogen, B. S., & Popescu, G. Highly sensitive quantitative imaging for monitoring single cancer cell growth kinetics and drug response. *PloS One.* **9** (2), e89000, (2014).
25. Mir, M., Tangella, K., & Popescu, G. Blood testing at the single cell level using quantitative phase and amplitude microscopy. *Biomedical Optics Express.* **2** (12), 3259-3266, (2011).
26. Park, Y. *et al.* Measurement of red blood cell mechanics during morphological changes. *Proceedings of the National Academy of Sciences of the United States of America.* **107** (15), 6731-6736, (2010).
27. Pham, H. V., Bhaduri, B., Tangella, K., Best-Popescu, C., & Popescu, G. Real time blood testing using quantitative phase imaging. *PloS One.* **8** (2), e55676, (2013).
28. Sridharan, S., Macias, V., Tangella, K., Kajdacsy-Balla, A., & Popescu, G. Prediction of prostate cancer recurrence using quantitative phase imaging. *Scientific Reports.* **5**, 9976, (2015).
29. Park, H. *et al.* Measuring cell surface area and deformability of individual human red blood cells over blood storage using quantitative phase imaging. *Scientific Reports.* **6**, 34257, (2016).
30. Bishitz, Y., Gabai, H., Girshovitz, P., & Shaked, N. T. Optical-mechanical signatures of cancer cells based on fluctuation profiles measured by interferometry. *Journal of Biophotonics.* **7** (8), 624-630, (2014).

